

Optimal control of a qubit coupled to a two-level fluctuator

P. Rebentrost,^{1, 2,*} I. Serban,^{1, 2} T. Schulte-Herbrüggen,³ and F.K. Wilhelm^{2, †}

¹*Department Physik, ASC and CeNS, Ludwig-Maximilians-Universität, Theresienstr. 37, 80333 München, Germany*

²*IQC and Department of Physics and Astronomy, University of Waterloo,
200 University Ave W, Waterloo, ON, N2L 3G1, Canada*

³*Department of Chemistry, Technische Universität München, Lichtenbergstrasse 4, 85747 Garching, Germany*

(Dated: February 9, 2020)

A central challenge for implementing quantum computing in the solid state is decoupling the qubits from the intrinsic noise of the material. We investigate limits of controllability for a paradigmatic model: A single qubit coupled to a two-level fluctuator exposed to a heat bath. We systematically search for optimal pulses using a generalization of the novel open system Gradient Ascent Pulse Engineering (GRAPE) algorithm. We show and explain that next to the known optimal bias point of this model, there are optimal shapes which refocus unwanted terms in the Hamiltonian. We study the limitations of control set by the decoherence properties in the fast flipping regime, which go beyond a simple random telegraph noise model. This can lead to a significant improvement of quantum operations in hostile environments.

A promising class of candidates for the practical realization of scalable quantum computers are solid state quantum devices based on superconductors [1, 2, 3, 4, 5] and lateral quantum dots [6]. A central challenge to overcome in this enterprise is the inevitable coupling to the macroscopic bath of degrees of freedom in the solid not used for quantum computation, which leads to decoherence (see e.g. Ref. [7] for a recent review). Many of these decoherence sources can be engineered at the origin. On the other hand, intrinsic slow noise originating from two level fluctuators (TLFs) is much harder to suppress at the source [8, 9], even though significant progress has also been made here [10, 11]. Thus, in order to advance the limitations of coherent quantum manipulations in the solid state, it is imperative to find strategies which accomodate this kind of noise. A number of methods have been proposed by intuition and analogies to different fields, such as dynamical decoupling [12, 13], the optimum working point strategy [1, 5, 14], and NMR-like tricks [15]. Even in light of their success, it is by no means clear, whether even better strategies can be formulated and, on a more general level, where the limits of quantum control under hostile conditions are reached. Thus we resort to numerical methods of optimal control. The GRAPE (gradient ascent pulse engineering) algorithm [16] has proven useful in coupled Josephson devices already [17, 18]. In this work, we extend its latest development, openGRAPE [19] to include complex environments encompassing a non-Markovian, non-Gaussian environmental degree of freedom — a single TLF coupled to a regular heat bath.

In the singular coupling relaxation regime with strictly Markovian physics, the wealth of optimal control was shown when encoding a logical qubit into several physical ones thus generalising decoherence-free subspace approaches [19]. Here, moving to non-Markovian and highly anisotropic relaxation mechanisms, the advantages will show up without encoding. We show that next to

the optimal point there is also an optimal gate duration and that accelerating the fluctuations can improve the gate. We discuss the physics ultimately limiting the gate performance no longer correctable by pulse shaping.

Model and method.—In macroscopic samples, there is ubiquitous [8, 9, 20] $1/f$ noise. The Dutta-Horn model [21, 22], explains this phenomenon by the (classical) superposition of TLFs which randomly jump between their states, a process known as random telegraph noise (RTN). In clean mesoscopic samples, discrete levels of the noise process from a single dominating fluctuator [1, 23] can be resolved. This leads to semi-phenomenological Hamiltonians [24, 25, 26].

We specifically model a qubit coupled to a single TLF by $\hat{H} = \hat{H}_S + \hat{H}_I + \hat{H}_B$, \hat{H}_S which itself is coupled by \hat{H}_I to a bath of harmonic oscillators \hat{H}_B acting as heat reservoir. We set

$$\hat{H}_S = E_1(t)\hat{\sigma}_z + \Delta\hat{\sigma}_x + E_2\hat{\tau}_z + \Lambda\hat{\sigma}_z\hat{\tau}_z, \quad (1)$$

with $\hat{\sigma}_i$ and $\hat{\tau}_i$ the usual Pauli matrices operating in qubit and fluctuator Hilbert space respectively. $E_1(t)$ is time-dependent and serves as an external control. The source of decoherence is the coupling of the TLF to the heat bath, which, for the TLF in isolation leads to incoherent transitions between the TLF eigenstates,

$$\hat{H}_I = \sum_i \lambda_i (\hat{\tau}^+ \hat{b}_i + \hat{\tau}^- \hat{b}_i^\dagger) \quad \hat{H}_B = \sum_i \hbar\omega_i \hat{b}_i^\dagger \hat{b}_i. \quad (2)$$

We introduce an Ohmic bath spectrum $J(\omega) = \sum_i \lambda_i^2 \delta(\omega - \omega_i) = \kappa\omega\Theta(\omega - \omega_c)$ containing the couplings λ_i , the dimensionless damping κ , and a high frequency cutoff ω_c .

We are interested in the qubit evolution in the limit of slow TLF flipping. For this purpose we use a standard master equation to describe the dynamics of the system qubit \otimes TLF. By keeping the impurity, we can treat this system consistently whereas tracing out the fluctuator in

this first step would lead to an intricate non-Markovian master equation. We perform a standard derivation of the Bloch-Redfield equation valid down to low temperatures in the motional narrowing limit [7, 27], which here requires $k_B T \gg \kappa E_2$. We obtain the generalized master equation

$$\begin{aligned} \dot{\hat{\rho}}_S(t) = & \frac{1}{i\hbar} [\hat{H}_S, \hat{\rho}_S(t)] + [\hat{\sigma}_1^+, \hat{\Sigma}_1^- \hat{\rho}_S(t)] + [\hat{\sigma}_1^-, \hat{\Sigma}_0^+ \hat{\rho}_S(t)] \\ & - [\hat{\sigma}_1^-, \hat{\rho}_S(t) \hat{\Sigma}_1^+] - [\hat{\sigma}_1^+, \hat{\rho}_S(t) \hat{\Sigma}_0^-] \end{aligned} \quad (3)$$

with the different rate tensors ($s = 0, 1$)

$$\hat{\Sigma}_s^\pm = \frac{1}{(i\hbar)^2} \int_0^\infty dt'' \int_0^\infty d\omega J(\omega) (n(\omega) + s) e^{\pm i\omega t''} \hat{\tau}^\pm(t'') \quad (4)$$

and $n(\omega)$ is the Bose function. Note, that this derivation treats the qubit-TLF interactions nonperturbatively, hence the various correlation matrices contain the full dynamics of the qubit-TLF system and do explicitly depend on the control $E_1(t)$ which is contained in eq. 4 through the interaction representation of the operators $\hat{\tau}^\pm$.

Our model goes far beyond a simple independent RTN assumption [13] and captures the correlations between qubit and TLF [24]. Still, it is useful to introduce the parameters of the RTN which would result for $\Lambda \rightarrow 0$. The TLF flipping rate is $\gamma = 2\kappa E_2 \coth(E_2/T) \ll E_2$, the sum of the excitation and relaxation rate. It enters the two-point noise spectrum of random telegraph noise

$$S_{\text{RTN}}(\omega) = \int_{-\infty}^\infty dt e^{-i\omega t} \langle \hat{\tau}_z^I(t) \hat{\tau}_z^I(0) \rangle_{\text{eq}} = \Lambda^2 \frac{\gamma}{\omega^2 + \gamma^2}. \quad (5)$$

This is the Fourier transform of the interaction representation of $\hat{\tau}_z$ taken in the interaction picture assuming the bath in equilibrium. In this limit, we can find relaxation rates $1/T_1 = \frac{\Lambda^2}{E^2} S(2E)$ and $1/T_2 = 1/2T_1 + \frac{E_1^2}{E^2} S(0)$ with $E = \sqrt{\Delta^2 + E_1^2}$. For our Hamiltonian, there is no entanglement between qubit and TLF created out of a factorized initial state, thus these are classical correlations.

We formulate the control approach by rewriting the master equation (3) as $\dot{\rho}(t) = -(i\mathcal{H}(E_1(t)) + \Gamma(E_1(t)))\rho(t)$ with the Hamiltonian commutator superoperator $\mathcal{H}(E_1(t))(\cdot) = [H(E_1(t)), \cdot]$ and the relaxation superoperator Γ , both time-dependent via the control $E_1(t)$. The formal solution to the master equation is a linear quantum map operating on the physical initial state according to $\rho(t) = F(t)\rho(0)$. Thus F itself follows the operator equation of motion

$$\dot{F} = -(i\mathcal{H} + \Gamma)F \quad (6)$$

with initial condition $F(0) = \mathbb{1}$ as in ref. [19]. The task is to find control amplitudes $E_1(t)$ with $t \in [0, T]$ and T being a fixed final time such that the dissipative time evolution $F(T)$ obeying Eqn. 6 comes closest to the target map F_U in the Euclidean distance

$$\|F_U - F(T)\|_2^2 = \|F_U\|_2^2 + \|F(T)\|_2^2 - 2 \text{Re} \text{tr}\{F_U^\dagger F(T)\}.$$

Clearly, this is the case, when the trace fidelity

$$\phi = \text{Re} \text{tr} (F_U^\dagger F(T)) \quad (7)$$

is maximal. Note, that in an open system, we cannot expect to achieve zero distance to a unitary evolution F_U [19], the goal is to come as close as possible.

We find these pulses by a gradient search. We digitize $F(T) \approx F_N \cdots F_j \cdots F_1$, where the interval $[0, T]$ is divided into N slices of duration Δt , one finds by Eqn. 6

$$F_j = e^{-\Delta t(i\mathcal{H}(E_1(j)) + \Gamma(E_1(j)))} \quad (8)$$

with $E_1(j)$ being the control amplitude in the j^{th} time slice. The gradient of the fidelity can be computed analytically as $\frac{\partial \phi}{\partial E_1(j)} = -\text{Re} \text{tr} \left(F_U^\dagger F_N \cdots F_{j+1} \Delta t \frac{\partial(i\mathcal{H}(E_1(j)) + \Gamma(E_1(j)))}{\partial E_1(j)} F_j \cdots F_1 \right)$.

We aim at optimizing the evolution of the qubit alone. Therefore, we trace out the TLF at the end of the full time evolution $F(T)$ retaining all degrees of freedom in the intermediate steps F_j , schematically

$$F^R = \text{tr}_{\text{TLF}} F(\rho_{\text{TLF}}^{\text{eq}}) \quad (9)$$

where the resulting map F^R acts on the space of qubit density matrices alone. Here, we assume standard factorized initial conditions with the fluctuator in equilibrium, $\rho(0) = \rho_Q \otimes \rho_{\text{TLF}}^{\text{eq}}$. We use F^R in the fidelity eq. (7) to optimize time evolution.

Results and their discussion.— Exploiting the above model, we now focus on optimizing controls for a Z -gate. In a single qubit the paradigmatic advantages are evident: (1) an error rate up to approx. one order of magnitude lower than the current “optimal working point strategies”; (2) the fidelities obtainable reach the T_1 limit of the relaxation model; (3) the optimized controls relate to optimal times via self-refocussing effects—thus showing how openGRAPE-derived controls provide physical insight even under advanced relaxation schemes. Similar findings are to be expected beyond one qubit gates.

An overview of the accessible gate performance as a function of the duration t_g of the gate is given in Fig. 1 (top). We notice that excellent gate performance can be achieved for pulse time $t_g \gtrsim \pi/\Delta$. This corresponds to the intrinsic drift induced by the static $\Delta\sigma_x$ performing at least a full loop around the Bloch sphere, hence removing unwanted free evolution. Indeed, we see on the Bloch sphere Fig. 2 right that at $t_g = 3.375/\Delta$, the pulse consists of half the z rotation, a full loop around x , and the second half of the z -rotation. At shorter times, the pulses cannot use the physical resource provided by the drift to refocus the qubit.

At longer times the gate performance mildly deteriorates, depending on the value of κ . This indicates that

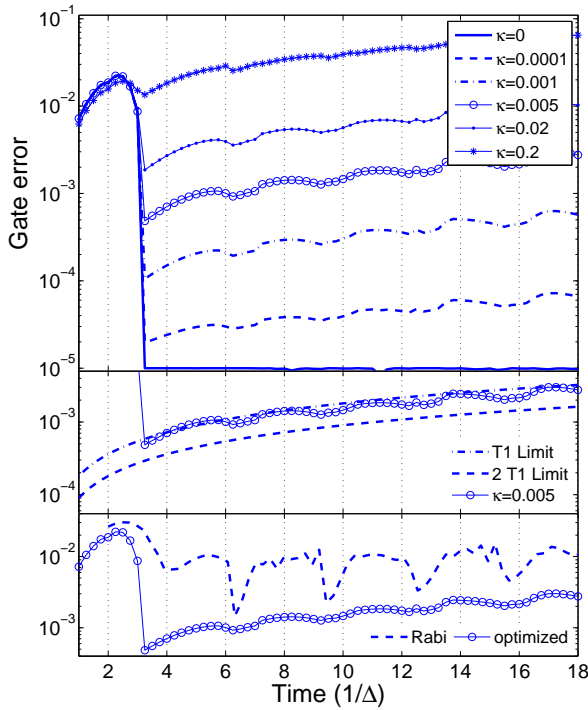


FIG. 1: Top: Gate error for optimal Z-gate pulses with different values of κ . There is a periodic sequence of minima around $t_n = \pi/\Delta$. Middle: The gate error of optimized pulses approaches a limit set by T_1 and $2T_1$ as shown with $\kappa = 0.005$. Bottom: Optimized pulses reduce the error rate by approximately one order of magnitude compared to Rabi pulses for $\kappa = 0.005$. In all figures the system parameters are $E_2 = 0.1\Delta$, $\Lambda = 0.1\Delta$ and $T = 0.2\Delta$.

the optimal pulses are essentially limited by T_1 processes at the optimal working point. We compare the performance to $1 - e^{-t_g/T_1}$ with T_1 obtained at $E_1 = 0$. The optimized pulses are able to beat this limit which indicates that $T_1(E_1)$ is a lower bound for the effective T_1 , see Fig. 1 (middle panel).

We also observe shallow minima of the error at gate times $t_n \approx n\pi/\Delta$, which are also explained by Fig. 2. At these t_n we have n rotations around x where the controls can be kept at the optimal point $E_1 = 0$. For slightly shorter/longer times we need to switch the controls on to accelerate/slow down the precession with a frequency $\Omega_p = 2\sqrt{\Delta^2 + (E_1 + \hat{\tau}_z\Lambda)^2}$ depending on the τ_z of the impurity, resulting in a tilted precession axis. These tilted axes are more sensitive to the TLF, as Ω_p depends on the flipping of τ_z at finite E_1 whereas at zero mean tilt, $E_1 = 0$, Ω_p is insensitive to the TLF. In Fig. 1 (bottom panel) we see that the performance of simple RF-pulses comes close to the optimized pulses at these t_n , in the closest case the errors are $(1 - \phi)_{\text{Rabi}} = 1.5 \cdot 10^{-3}$ and $(1 - \phi)_{\text{Graep}} = 0.9 \cdot 10^{-3}$. It remains far, up to an order of magnitude, at other times. In other words,

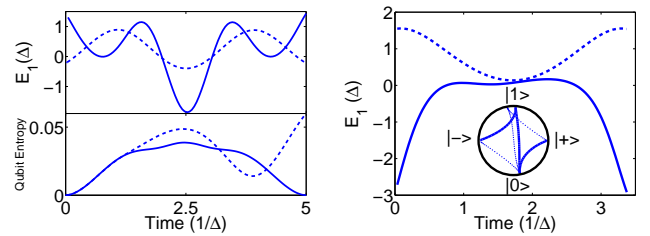


FIG. 2: Left: Comparison of pulse shape and qubit entropy between Rabi (---) and optimized pulse (—) at $t_g = 5/\Delta$ and $\kappa = 0$; Right: Rabi (---) and optimized pulse (—) at $t_g = 3.375/\Delta$ and $\kappa = 0.05$. Inset shows the evolution of initial state $\rho = |+\rangle\langle+|$, $|\pm\rangle = (|0\rangle \pm |1\rangle)/\sqrt{2}$ on the Bloch sphere under these pulses. $T = 0.2\Delta$, $E_2 = 0.1\Delta$, $\Lambda = 0.1\Delta$ in all panels.

the narrow and deep minima of the error for the regular Rabi pulse become shallow and broad by using GRAPE. Thus, the pulse optimization allows to at least approximately redirect the Δ drift even outside the t_n , whereas the Rabi pulses let them go. In the co-rotating frame typically used for describing Rabi pulses, the source of error is essentially the fast oscillating counter-rotating component, which is significant when using these short, high-amplitude pulses which only consist of a few carrier periods.

We now analyze the dependence on the bath parameters. In Fig. 3 we can identify a nonmonotonic dependence of the error of the ideal pulse on γ , which seems to be counterintuitive at first, but is readily understood in physical terms. At low γ , we can approximate $(1 - \phi) = a + b\gamma$. The linear growth with γ accounts for the increasing probability for the TLF to flip at a random time during the evolution. This is reflected in the power spectrum of the RTN for low γ , where essentially $S(\omega > \gamma) \simeq \Lambda^2\gamma/\Delta^2$, Eq. 5. Note that for time-independent E_2 and very long evolution, T_2 would be dominated by $S(0)$ in the Markovian limit, however, at very fast manipulations through an external field, the environment is only sampled at higher frequencies, $\omega > \gamma$. The coefficient $a \simeq 0$ reflects, that at $\gamma = 0$, no entropy flows from the fluctuator to the qubit — the GRAPE pulse fully compensates for the fact that we do not know which state the TLF is in, as long as it remains in that state.

On the other hand, for a high flipping rate γ , the physics of motional narrowing sets in, which limits the low frequency noise and hence the pure dephasing to $S_{\text{RTN}}(\omega < \gamma) = \Lambda^2/\gamma$ which vanishes for $\gamma \rightarrow \infty$. Indeed, the high- γ part of the error is described by a law $c + d/\gamma$. The again finite limiting value c again captures the residual decoherence which occurs even if the RTN model Eq. (5) suggests absence of noise.

Consequently, there is a γ_{max} at which the error is maximum. Remarkably, $\gamma_{\text{max}} \simeq 0.32\Delta \simeq \Delta/\pi$ indepen-

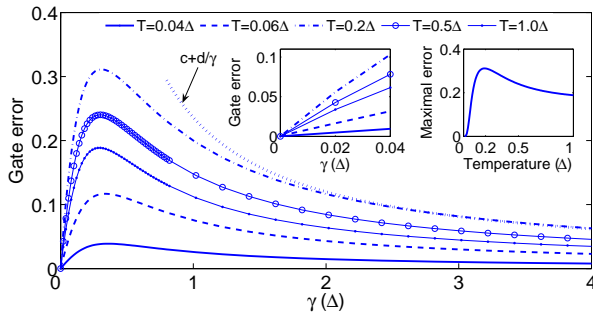


FIG. 3: Gate error versus TLF rate γ for various temperatures for a long optimized pulse ($t_g = 60/\Delta$, $E_2 = 0.1\Delta$ and $\Lambda = 0.1\Delta$). A high γ fit with $d/\gamma + c$ is also pictured. The left inset is a magnification of the low γ part of the main plot and reveals the linear behaviour. The right inset shows the maximum of the curves versus temperature.

dent of any other parameters such as temperature and pulse length: The performance is worst if the TLF flips roughly once per free rotation around x .

The maximal amplitude of the error $E_{\max} = (1 - F)(\gamma_{\max})$ as well as most other fit parameters show a non-monotonic temperature dependence, exponentially suppressed at low T and saturates to a finite high-temperature limit. The intermediate maximum can be related to the maximum of the equilibrium susceptibility of the TLF, which is maximum at $T \simeq 2E_2$. The more responsive the TLF is to perturbations of its z -field, the stronger it will influence the qubit.

Comparison to other work.— Similar systems have been addressed before, however, either studying decoherence without controls (e.g. [24, 26]) or finding refocusing sequences by ingenuity rather than optimization [12, 13], which also holds for optimal working-point strategies [5, 14]. Comparing our advanced TLF model to the simpler one of a telegraph process [18] with $E_2 = 0$ (thus equal probabilities for both states) shows the latter cannot capture physical limitations at the large γ end. Neither periodicity of optimum times has been discussed. A similar approach for two qubits and classical $1/f$ noise has been taken in Ref. [28]. In the final stages of finishing this work, a related model has been addressed [29], without heat bath. Consequently it makes no reference to the entropy of the initial state of the TLF nor to the dependence on γ . Moreover, though obtaining optimal times from revivals of the system, it neither predicts their details nor their sensitivity to κ .

Conclusion.— We have investigated a central model for decoherence in solid-state systems, a qubit coupled to a two-level fluctuator which itself is coupled to a heat bath. Our study is the first to exploit the explicit dynamics of a complex non-Markovian environment in optimal control of open systems for implementing quantum gates. For a wide range of parameters, we have identified

self-refocusing effects, which are usually only visible at specific optimal pulse durations but can now be achieved more robustly. We have shown that both for fast and slow flipping of the TLF high-fidelity control can be achieved. Some of these aspects are not captured in simpler random telegraph noise models.

We gratefully acknowledge support by NSERC discovery grants, by the EU in the projects EuroSQIP and QAP as well as by the DFG through SFB 631.

* Electronic address: prebentrost@iqc.ca

† Electronic address: fwilhelm@iqc.ca

- [1] P. Bertet, I. Chiorescu, G. Burkard, K. Semba, C. J. P. M. Harmans, D. P. DiVincenzo, and J. E. Mooij, Phys. Rev. Lett. **95**, 257002 (2005).
- [2] O. Astafiev, Y. Pashkin, T. Yamamoto, Y. Nakamura, and J. Tsai, Phys. Rev. B **69**, 180507(R) (2004).
- [3] R. Simmonds, K. Lang, D. Hite, D. Pappas, and J. Martinis, Phys. Rev. Lett. **93**, 077003 (2004).
- [4] A. Wallraff, D. Schuster, A. Blais, L. Frunzio, R. Huang, J. Majer, S. Kumar, S. Girvin, and R. Schoelkopf, Nature **431**, 162 (2004).
- [5] D. Vion, A. Aassime, A. Cottet, P. Joyez, H. Pothier, C. Urbina, D. Esteve, and M. Devoret, Science **296**, 286 (2002).
- [6] T. Hayashi, T. Fujisawa, H. Cheong, Y. Jeong, and Y. Hirayama, Phys. Rev. Lett. **91**, 226804 (2003).
- [7] F. Wilhelm, U. Hartmann, M. Storcz, and M. Geller, quant-ph/0603637 (unpublished).
- [8] S. Jung, T. Fujisawa, and Y. Hirayama, Appl. Phys. Lett. **85**, 768 (2004).
- [9] A. Zorin, F. Ahlers, J. Niemeyer, T. Weimann, H. Wolf, V. Krupenin, and S. Lotkhov, Phys. Rev. B **53**, 13682 (1996).
- [10] J. Eroms, L. van Scharenburg, E. Driessens, J. Plangenberg, C. Huizinga, R. Schouten, A. Verbruggen, C. Harmans, and J. Mooij, Appl. Phys. Lett. **89**, 122516 (2006).
- [11] M. Steffen, M. Ansmann, R. McDermott, N. Katz, R. Bialczak, E. Lucero, M. Neely, E. Weig, A. Cleland, and J. Martinis, Phys. Rev. Lett. **97**, 050502 (2006).
- [12] L. Faoro and L. Viola, Phys. Rev. Lett. **92**, 117905 (2004).
- [13] H. Gutmann, W. Kaminsky, S. Lloyd, and F. Wilhelm, Phys. Rev. A **71**, 020302(R) (2005).
- [14] G. Ithier, E. Collin, P. Joyez, P. Meeson, D. Vion, D. Esteve, F. Chiarello, A. Shnirman, Y. Makhlin, J. Schrieffl, and G. Schön, Phys. Rev. B **72**, 134519 (2005).
- [15] E. Collin, G. Ithier, A. Aassime, P. Joyez, D. Vion, and D. Esteve, Phys. Rev. Lett. **930**, 157004 (2004).
- [16] N. Khaneja, T. Reiss, C. Kehlet, T. Schulte-Herbrüggen, and S. Glaser, J. Magn. Res. **172**, 296 (2005).
- [17] A. Spörl, T. Schulte-Herbrüggen, S. Glaser, V. Bergholm, M. Storcz, J. Ferber, and F. Wilhelm, quant-ph/0504202 (unpublished).
- [18] M. Möttönen, R. de Sousa, J. Zhang, and K. Whaley, Phys. Rev. A **73**, 022332 (2006).
- [19] T. Schulte-Herbrüggen, A. Spörl, N. Khaneja, and S. Glaser, quant-ph/0609037 (unpublished).
- [20] D. J. van Harlingen, T. L. Robertson, B. L. Plourde, P.

Reichardt, T. Crane, and J. Clarke, Phys. Rev. B **70**, 064517 (1988).

[21] P. Dutta and P. Horn, Rev. Mod. Phys. **53**, 497 (1981).

[22] M. Weissman, Rev. Mod. Phys. **60**, 537 (1988).

[23] R. Wakai and D. van Harlingen, Phys. Rev. Lett. **58**, 1687 (1987).

[24] E. Paladino, L. Faoro, G. Falci, and R. Fazio, Phys. Rev. Lett. **88**, 228304 (2002).

[25] R. de Sousa, K. Whaley, F. Wilhelm, and J. von Delft, Phys. Rev. Lett. **95**, 247006 (2005).

[26] A. Grishin, I. V. Yurkevich, and I. V. Lerner, Phys. Rev. B **72**, 060509 (2005).

[27] R. Alicki, D. Lidar, and P. Zanardi, Phys. Rev. A **73**, 052311 (2006).

[28] S. Montangero, T. Calarco, and R. Fazio, quant-ph/0611166 (unpublished).

[29] M. Grace, C. Brif, H. Rabitz, I. Walmsley, R. Kosut, and D. Lidar, quant-ph/0611189 (unpublished).